HIERARCHAL STRUCTURES OF SILICON AND GERMANIUM NANOWIRES FOR LITHIUM ION BATTERIES

A Thesis

Presented to the Faculty of the Graduate School

of Cornell University

In Partial Fulfillment of the Requirements for the Degree of

Master of Science

by

Victor R. Lambert

August 2016

ABSTRACT

Lithium alloying materials like silicon and germanium have garnered much attention since they exceed the charge capacity of currently used graphite anodes by up to tenfold. However, these materials expand up to 400% upon lithiation, causing material pulverization and significant capacity loss. Nanostructuring has proven to mitigate the pulverization issue by allowing the material to withstand the internal stresses of volume expansion. Nanowires possess attractive qualities for batteries, including low diffusion length of lithium ions and efficient one dimensional electron conduction. Richards *et al* have demonstrated a supercritical fluid synthesis to grow silicon and germanium nanowires directly on metal films, eliminating the need for binder and conducting additive. Nanowire films grown on nickel foams exhibit high loadings of up to 5 mg/cm^2 while maintaining electrochemical performance. Similar synthesis conditions used with planar substrates allows for direct comparison of rate performance of a three dimensional structure and a planar structure.

BIOGRAPHICAL SKETCH

Victor Lambert received his BS in chemical engineering from Northeastern University in May 2014. While studying for his bachelor's degree, Victor worked as an intern for several energy related companies including Nuvera Fuel Cells, 1366 Technologies, and Ambri inc. Victor continued his study of the energy industry at Cornell University as an Earth-Energy Systems NSF IGERT trainee, eventually finishing his MS in chemical engineering and graduating in August 2016.

Dedicated to my friends and family for their constant support.

ACKNOWLEDGEMENTS

I would like to thank my advisor Tobias Hanrath for all his help throughout the research process. I also acknowledge my committee, Professors Hector Abruña and Yong Joo for their support. This work made use of the Cornell Center for Materials Research Shared Facilities which are supported through the NSF MRSEC program (DMR-1120296). I acknowledge financial support from the NSF IGERT program (DGE-0966045).

TABLE OF CONTENTS

LIST OF FIGURES

INTRODUCTION

Secondary batteries are used in many forms of modern technology, from mobile phones to electric vehicles. Lithium ion batteries (LIB) represent the current state of the art for energy density, specific energy, and slow self-discharge.[1] Though LIBs represent the result of many years of research, they do not possess the energy density to be competitive with liquid fuels such as gasoline. Battery capacity is the limiting factor of the range of electric vehicles, one primary obstacle for increased adoption. If the global transportation system is to shift away from fossil fuels, higher capacity batteries must be developed. The capacities of state of the art batteries are limited by the fundamental properties of the materials used, it is impossible to make significant advances in energy density without incorporating new materials.[1] Modern lithium-ion batteries use graphite as an anode and lithium cobalt oxide as a cathode.[1,2] Graphite is intercalation anode, where the lithium ions move in and out of the spaces between the carbon layers. It has a theoretical maximum specific energy of 372 mAh/g. Alloying materials, including silicon and germanium, have significantly higher specific capacities than graphite.

Promising anode materials include silicon and germanium, having significantly higher energy density and specific energy than graphite.[3-5] Silicon, with a room temperature specific capacity of 3579 mAh/g, has a theoretical capacity more than ten times higher than graphite.[6] Germanium, though less than silicon, has a much higher capacity

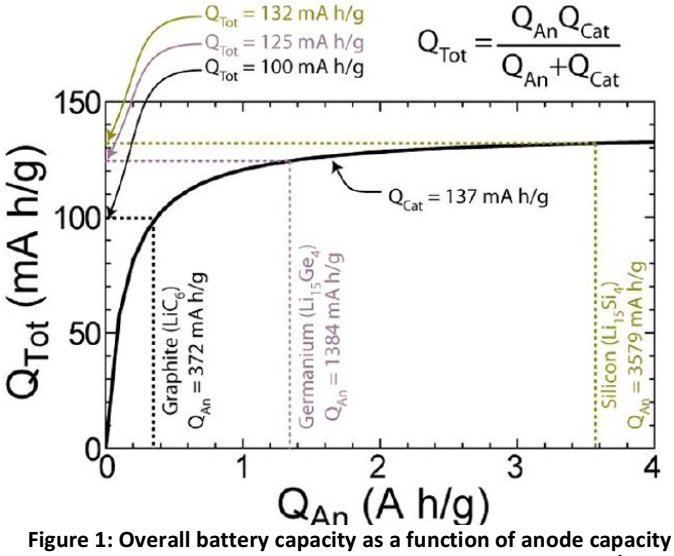

Figure 1: Overall battery capacity as a function of anode capacity with a cathode capacity of lithium cobalt oxide, 137 mAhg^{-1}. Figure adapted from Chockla *et al.*

than graphite of 1384 mAh/g. The two materials also have similar volumetric capacities, 8334 mAh/mL for silicon and 7366 mAh/mL for germanium.[6] Figure 1 shows the capacity of a full battery cell built using cobalt oxide cathode as a function of anode capacity. The total capacity increases slowly because the total capcity of a full cell depends primarily on the capacity of the less charge dense material. Marked on the graph is a comparison to the capacity of a state of the art lithium ion battery today and the overall capacity that could be achieved with silicon and germanium anodes. Silicon could provide an increase of about 30% over the current state of the art, and germanium could provide an increase of 25%.[4] Germanium is significantly more expensive than silicon, however it comes with several distinct advantages. Silicon is not very electrically conductive, germanium has higher conductivity and over 400 times faster diffusion of lithium ions.[7] This faster diffusion and higher conductivity results in much better performance at higher charging and discharging rates than silicon batteries. Both Silicon and germanium have low potentials vs. Li/Li^+, silicon having a discharge potential ranging from 20-300mV.[8] This corresponds to a voltage of about 3.5-4.0V with a NMC cathode.[9] Though these materials show significant promise, there are several drawbacks that must be overcome in order to reach widespread usage.

Silicon and germanium expand significantly upon lithiation, 280% for silicon and 200% for germanium, which results in pulverization as the battery cycles.[6] Lithiation proceeds as a two phase system, the volume increasing as the fraction of material fully lithiated increases. The deeper the electrode is cycled, the larger the final volume. When material pulverization occurs, some of the electrode is no longer electrically connected to the battery, rendering that portion of the material inactive and lost as electrical capacity. In addition to material pulverization, silicon electrodes can

change morphology and shape with the expansion and shrinking, resulting in further detachment and capacity fade. While cycling vs lithium, below 1V vs Li/Li^+, decomposition of organic electrolyte components occurs.[10,11] This results in the formation of a layer on the surface, called the solid-electrolyte interface (SEI). The ideal SEI is electrically insulating to prevent the further decomposition of electrolyte, and ionically conducting to allow the facile movement of ions through the battery.[12]

Nanoscale features have demonstrated the ability to better accommodate the stresses of volume change and mitigate the pulverization of the electrode.[12] A variety of structures have been proposed for the structure, including thin films, particles, and wires.[12-14] Figure 2 demonstrates the effects of cycling on different silicon structures.[3] Nanowires with a diameter of less than 300 nanometers have demonstrated the ability to withstand the pulverization effect of cycling.[15] Efficient 1D transport of electrons along the length of the wire, along with the high surface area, helps increase the rate of charge and discharge.

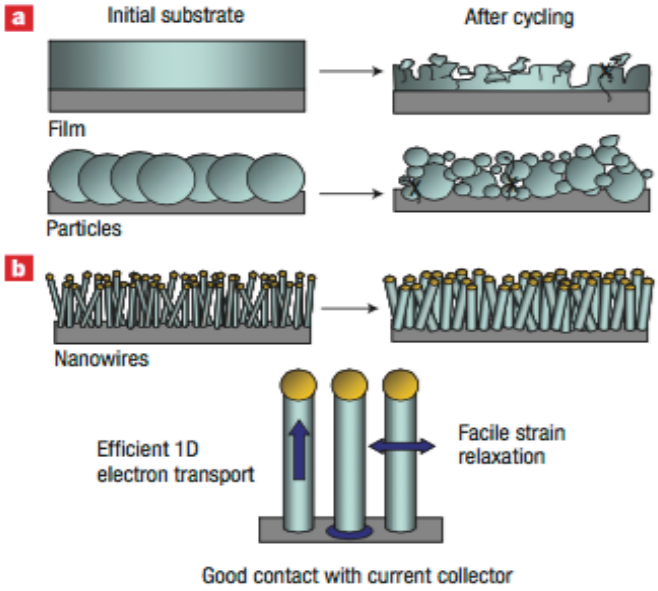

Figure 2: a) Pulverization of particles and films upon cycling b) nanowires survive expansion. Figure adopted from Chan *et al*

Though nanowires present a very attractive material for silicon and germanium anodes, there are several significant obstacles to increased adoption. Nanowires are difficult to synthesize, and most

current methods are too expensive to create the many kilograms of nanowires necessary for industrial scale. When expanding, nanowires directly connected to the surface experience localized force at the substrate interface. Nanoscale features on the substrate may help to accommodate this force. During large volume changes of cycling, the SEI can crack, this results in more capacity loss as the SEI reforms leading to further capacity loss.[16] Formation of a stable SEI layer is essential for long term cycling of a silicon or germanium battery. Tailoring of the surface of the nanowires and the electrolyte components can stabilize this interfaces.[17-19] These two interfaces, the wire/substrate and wire/electrolyte interfaces, are critical to the design of nanowire electrodes.

BACKGROUND

Silicon has long been recognized as having very high capacity to store lithium ions, and is seen as potential replacement for graphite. Nanostructuring has proven to be an effective method for mitigating the central problem of pulverization, though several problems still exist for nanowires.[3] Figure 3 shows a simplified version of a nanowire being lithiated, note that the SEI cracks during cycling and that there is significant stress at the base of a directly attached nanowire. Below are reviewed silicon nanowire electrochemical performance, and several common synthesis routes for silicon and germanium nanowires. The following discussion will touch on several techniques used to mitigate capacity fade and poor rate performance, and to highlight recent developments with germanium nanowires.

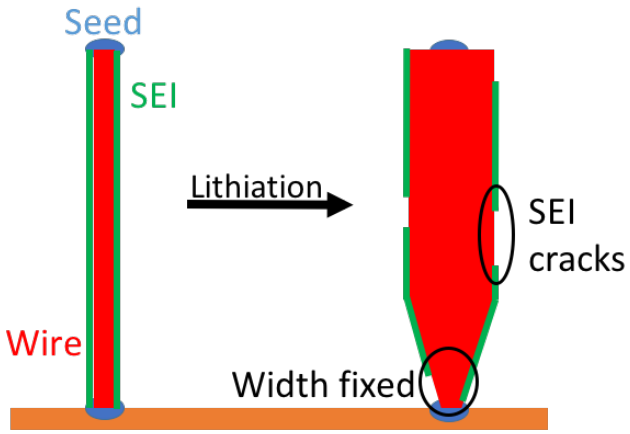

Figure 3: Problems associated with lithiation of direct attached silicon nanowires. Of particular note are SEI cracking and mechanical stability at the substrate/nanowire interface

Silicon Nanowire Performance

When silicon is lithiated, during the first discharge crystalline silicon converted to amorphous silicon at a phase boundary. This manifests as a long, sloping profile; The boundary between the two phases shifts, causing the potential to shift.[20] For the first cycle, the potential window is about 0.1V to 0V, and for later cycles this increases to about 0.5V to 0V. At room temperature, silicon can be lithiated until there are 3.75 lithium atoms per silicon atom, resulting in a lithium silicon intermetallic compound $Li_{15}S_4$. This phase corresponds to the actual room temperature value for the theoretical capacity, 3579 mAh/g, not the oft reported 4200 mAh/g, only reached above 400ºC.[21] The electrical conductivity of the amorphous silicon formed after the initial lithiation is the rate-limiting component of the electrode. With the poor conductivity, to get performance close

to the theoretical capacity it is necessary to cycle at very low rates, approximately C/20. Chan *et al.*, in one of the initial demonstrations of silicon nanowires, grown via the vapor-liquid-solid method with chemical vapor deposition, show a useable capacity of 3000 mAh/g.[3] The drawbacks of this scheme are the lack of scalability and the low areal mass loading of the samples. Solution grown nanowires, on the other hand, have the potential to have much higher mass loadings through slurry coating. Although the loadings are better, the overall performance was shown to be lower with a specific capacity of only 1500 mAh/g using supercritical fluid liquid solid (SFLS) synthesis.[22] These two results also demonstrate only performance for about 10 cycles.

Nanowire Synthesis

The most prominent bottom-up method is arguably the vapor-liquid-solid (VLS) mechanism based on seminal studies of gold nucleated silicon whiskers by Wagner and Ellis in the 1960s.[23] Interest in semiconductor NWs was rekindled in the late 90s when Lieber and co-workers demonstrated growth of nanometer diameter Si and Ge NWs from iron silicide clusters[24] and later gold seeds.[25] An interesting new direction in semiconductor NW synthesis methods emerged from the recent work of Ryan and co-workers who demonstrated that Ge NWs can also be grown directly on Cu films.[26] Yuan *et al.*[27] showed that single crystalline Si nanowires can be synthesized on the surface of various bulk metals including Ag, Al, Cu, Fe, Ni, Pb,

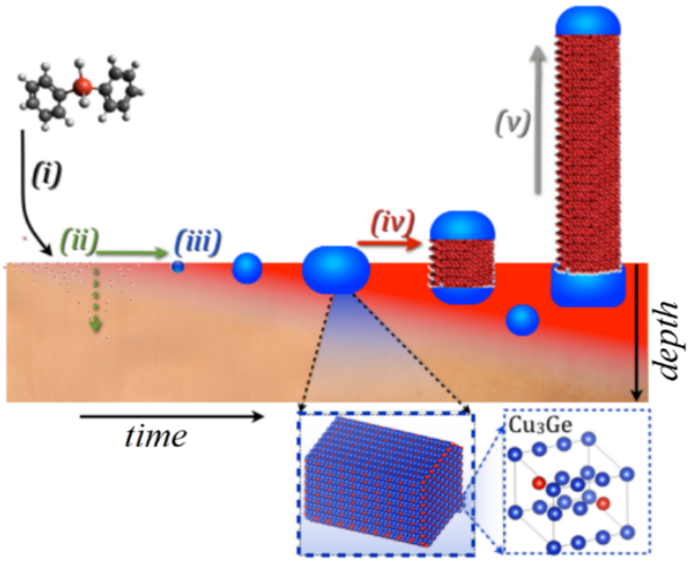

Figure 4: Wire growth mechanism depicted for germanium nanowires on a copper surface. Precursor first diffuses to the surface, then forms a germanide seed. The nanowire then grows from the seed.

and Ti. The shift from noble metal nanoparticle seeds to low-cost bulk films has important practical implications for electronic applications as well as the scalable and economical NW fabrication.

Another promising growth method has been investigated by Richards *et al.*, where wires are grown directly on a metal film at atmospheric pressure.[28] Copper is often used as a metal catalyst, deposited via metal evaporation on a stainless steel sheet. Figure 4 shows the mechanism of the process, where an organosilane or organogermane precursor decomposes at the surface, causing silicon or germanium to diffuse into the metal and to form copper silicide or germanide seed. Growth then proceeds from this seed, resulting in nanowire formation.[28] Substrates produced using this method can have areal loadings of up to 5 mg/cm^2. One drawback of many synthesis methods for nanowires is that they are not scalable enough to produce the quantities or loadings necessary for industrial production. For example, a typical electric vehicle requires about 10kg of nanowires, and most published synthesis methods are on the order of milligrams. Different from CVD or supercritical fluid reactors, direct growth could easily be scaled up using a roll-to-roll system and demonstrates higher loading.[28] Recently, very high loadings of up to 3.8 mg/cm^2 were reported using a tissue-like three-dimensional substrate to greatly increase the available growth area. Slurry coating can be used to accurately tune the loadings, and is often paired with solution growth methods. However, utilizing slurry coating adds processing steps and reduces the potential specific capacity of the electrode. Also, using slurry coating does not provide the added benefit of direct electrical contact with the surface.[29]

Electrolyte Additives

SEI formation and cracking results in substantial capacity fade, and the electrolyte must be tailored to provide a more flexible layer. Ideally, the SEI will be electrically insulating and conductive to

lithium ions, while still able to withstand the mechanical stresses of volume change. Typical electrolyte components are ethylene carbonate, diethylene carbonate, and $LiPF_6$.[20] These compounds break down into carbonates and lithium fluoride salt in the SEI layer during the first cycle in an irreversible reaction. Each cycle, the SEI cracks and more silicon is exposed to the electrolyte. This silicon reacts irreversibly with the electrolyte, resulting in capacity loss.[16] The composition and morphology of the SEI are directly related to the composition of the electrolyte. Several additives have proven to be effective at forming a more stable SEI layer, including fluoroethylene carbonate (FEC) and vinylene carbonate (VC). FEC, when used with silicon, has been shown to significantly increase the reversible capacity when used in small concentrations in the electrolyte (about 3%).[30] This is a result of the higher Li ion conductivity and less porous layer formed when FEC is used.[31] VC has also been shown to significantly improve both the fade rate and coulombic efficiency of half cells.[32] Although many results indicate that carbonate additives improve electrolyte performance, there is still not a good understanding of why the performance is improved. There is some evidence that native oxide plays a role in the initial formation of the SEI, where the Si-O bonds would be what initially breaks down to form the decomposition produces.[15,17] Optimization of electrolyte chemicals and additives is instrumental in creating a stable silicon or germanium anode.

Germanium Nanowire Performance

Several good results have been demonstrated with germanium nanowires, with different electrolyte compositions. Solution grown Ge nanowires, demonstrated by Chokla *et al*., were slurry coated

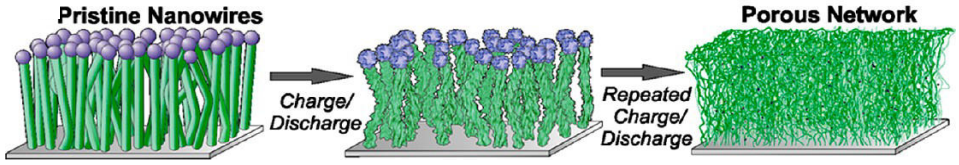

Figure 5: Germanium nanowires become a mesh upon cycling, taken from Kennedy *et al.*

onto coin cell substrates and cycled with several different electrolytes. The electrolyte demonstrated excellent performance, maintaining a stable capacity of 1248 mAh/g after 100 cycles with the addition of FEC in the electrolyte.[4] The electrode even shows 600 mAh/g capacity after 1200 cycles at a 1C rate. The anode even has the ability to discharge with appreciable capacity at very high rates, up to 10C.[4] Another promising result comes from Kennedy *et al*., where germanium nanowires were grown directly on a tin film and cycled for over 1000 cycles, demonstrating a final reversible capacity of 866 mAh/g.[33] VC was added to the electrolyte, which changed the morphology of the final structure. With VC, the germanium nanowires transformed into a porous mesh, shown in Figure 5.The nanowires splinter and merge during cycling with lithium, which prevents the loss of electrical contact from any wire which would have broken.[33] This morphology change was only observed when VC was added to the electrolyte. Otherwise, the wires disintegrated and did not have good performance. Germanium nanowires have lower capacity, but rate performance orders of magnitude higher than silicon wires.[4,26,33]

Hierarchal Structures

Although silicon and germanium nanostructures demonstrate good performance in planar films, many published results have extremely low loading. High mass loadings of silicon and germanium films result in high capacity fade because of material fracture and morphology change or low rate performance resulting from low conductivity of active material. One strategy to improve mass transfer, kinetic limitations, and low areal loading is to increase the effective area of the electrode by making a three-dimensional heterostructure. In contrast to a typical planar electrode, a 3D electrode has an additional shape on which the active material is placed. A 3D heterostructure allows for electronic connection to a greater proportion of the sample as well as facilitating rapid mass transfer of ions and expansion of silicon. Lee *et al* demonstrated that nanostructured

germanium on a nanostructured copper network has excellent electrochemical rate performance.[34] The device had loadings of up to 6 mg/cm^2 and demonstrated minimal loss of capacity at rates as high as 2 mAh/cm^2.[34] Also, three dimensional tissue like silicon nanowires have been shown to have a capacity of over 400 mAh/g in a full cell with a lithium iron phosphate cathode in addition to having a capacity of 3000 mAh/cm^2 at 1mA/cm^2.[29] Another interesting way to create a hierarchally structured electrode is to take a material which already has a three dimensional structure and deposit active material atop that.

A nickel foam provides an attractive, stable, high surface area substrate for the creation of a three-dimensional hierarchally structured electrode. Recently, several reports of material deposition on nickel foams have been published demonstrating its potential use in supercapacitive applications.[35,36] In principle, growth of silicon and germanium nanowires should be possible on a nickel foam. The additional surface area would allow for higher loadings to be reached and help alleviate the kinetic limitations of lithiation in silicon and germanium anodes. Utilizing a nickel foam also allows for easy comparison to planar substrates to quantify the improvement in performance.

Impedance Analysis of Nanowires

Impedance analysis is often used to determine kinetic limitations in battery electrodes. The technique applies a small ac voltage to the cell and records the impedance at each frequency. It can be used to extract parameters relevant to cell performance such as solution resistance and double layer capacitance if the spectra are fit to an accurate model. Early works on silicon nanowire impedance used standard parameters for fitting, and found that there was not an excellent fit in the low frequency regimes.[37] Typical models use a Warburg impedance element or a tangent element

to represent the capacitive blocking of the center of the nanoparticles, however this does not take into account size or morphology of the film. Bazant *et al* developed an impedance model for films of nanoparticle or nanowire electrodes from first principles of diffusion. In solving the diffusion equations for different geometries, he was able to account for both the curvature of the particles and for a distribution of particle sizes in the sample.[38] The impacts of changing these parameters is shown in Figure 6. The change in particle shape has a relatively small effect, slightly reducing the transition from Warburg to capacitive regime (impedance goes to infinity). Increasing standard deviation causes the diffusion impedance to slope more, rather than go to infinity (capacitive blocking) or pin at a 45-degree slope (Warburg).

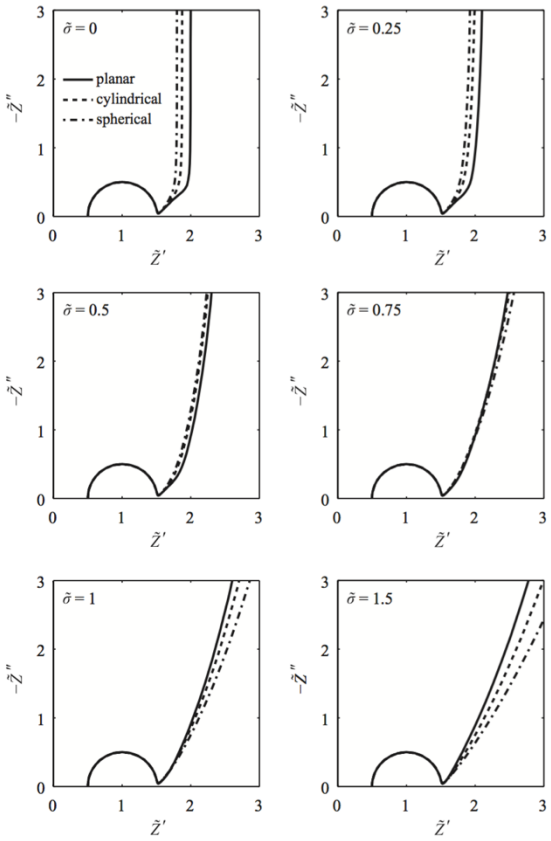

Figure 6: Impedance analysis taken from Bazant et al, note the difference in the diffusion element based on the shape and standard deviation of the nanoparticles

Preliminary battery data

Most of the initial work was applying the principles of battery testing to nanowires produced using direct growth, specifically the batch inductive method pioneered by Richards *et al*.[28] These wires present an attractive material for battery anodes for lithium ion batteries because they have loadings of 3-8 mg/cm^2, ideal for modern lithium ion batteries. Though there had been previous battery work in the Hanrath group, very little battery characterization had been completed on nanowire films. Germanium nanowires were assembled in a coin cell using a porous glass separator, 1M $LiPF_6$ in 1:1 EC/DEC electrolyte and tested at a C/10 rate. Initial cells, though they cycled, achieved much less than the theoretical capacity of germanium. Several process changes allowed more accurate loading measurement of the samples. After making these process changes, cells with close to the expected capacity were constructed; a representative charge capacity plot is shown in Figure 7. The initial capacity, though slightly lower than the theoretical capacity is still on par with the majority of literature values. Coulombic efficiency is low for the first cycle, which is expected because the nanowires transition from a crystalline to amorphous structure[39], and the SEI layer forms. The efficiency then recovers to a more reasonable value but begins to decline as the cell cycles. This indicates increasing amounts of secondary

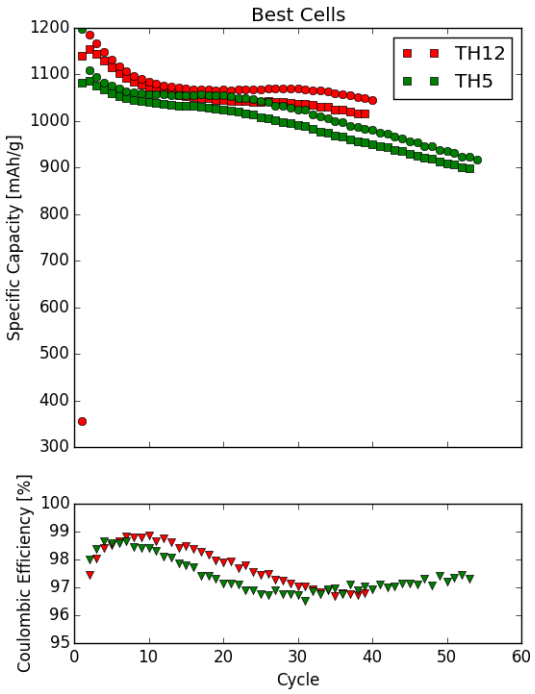

Figure 7: The best cells built during the initial testing of batch inductive grown germanium nanowires. They show initial capacity close to the theoretical limit.

reaction taking place. In addition, the fade rate is slightly higher than expected. This could be a result of the lack of VC or FEC in the electrolyte, both of which produce excellent results in literature.

Though performance of several cells was good, with initial capacities close to the theoretical capacity of germanium, several questions remain unanswered. The performance of the cells seems to be strongly loading dependent, as shown in Figure 8. There is a clear trend in that the lower loading samples often have a capacity much closer to the theoretical limit. The limitations of the scale and loading calculation are close to 0.5 mg, which means there is significant potential for error. If the mass of the samples is underestimated, then the specific capacity will be inflated from the actual value. In addition to questions on the importance of loading, only preliminary data have been collected for rate performance and varying electrolytes.

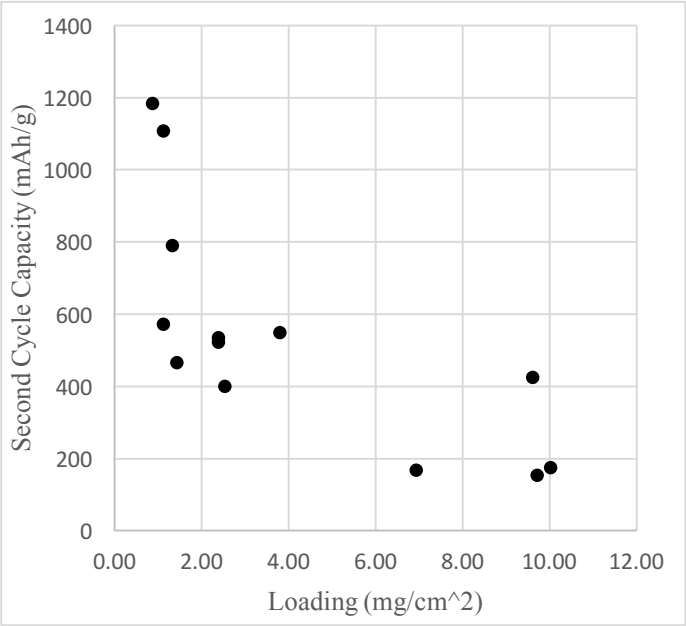

Figure 8: Loading in mg/cm2 plotted against second cycle capacity, there is a clear trend that higher loading is corrolated with lower specific capacity.

Battery impedance analysis

In addition to capacity and rate cycling data, some preliminary impedance spectra were also collected. Two germanium nanowire samples were prepared using the batch inductive method – resulting in very uniform coverage and morphology. The loading also was uniform between the samples, at 2.0 and 2.2 mg/cm^2. The morphology was similar to those shown above in the initial battery work section, although the wires were slightly larger than typical nanowire morphologies with a diameter of about 1 micron.

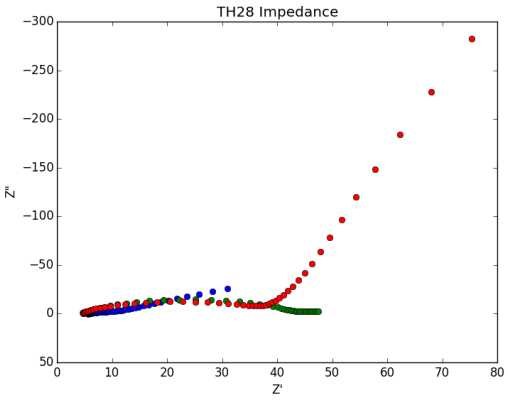

Figure 9: Impedance analysis of representative sample before cycling (red), after first lithiation (blue), and after the first delithiation (green).

The samples were then used to construct two coin cells, using 1M $LiPF_6$ in EC:DEC as the electrolyte. Impedance scans were conducted before cycling, after the first lithiation, and after the first delithiation. The results are summarized in Figure 9. The impedance in the delithiated state shows a single RC semicircle followed by a diffusion impedance. Delithiated states (red and green) also have a much higher impedance than the fully lithiated state, with a charge transfer resistance of about 40 ohms. The series resistance of all three scans is about five ohms. Though the scans at the beginning and end of each cycle show interesting information, much more information could be gained by conducting scans within a cycle. Also, impedance analysis is best conducted at equilibrium (after the initial formation of the SEI), so it is beneficial to wait a few cycles.

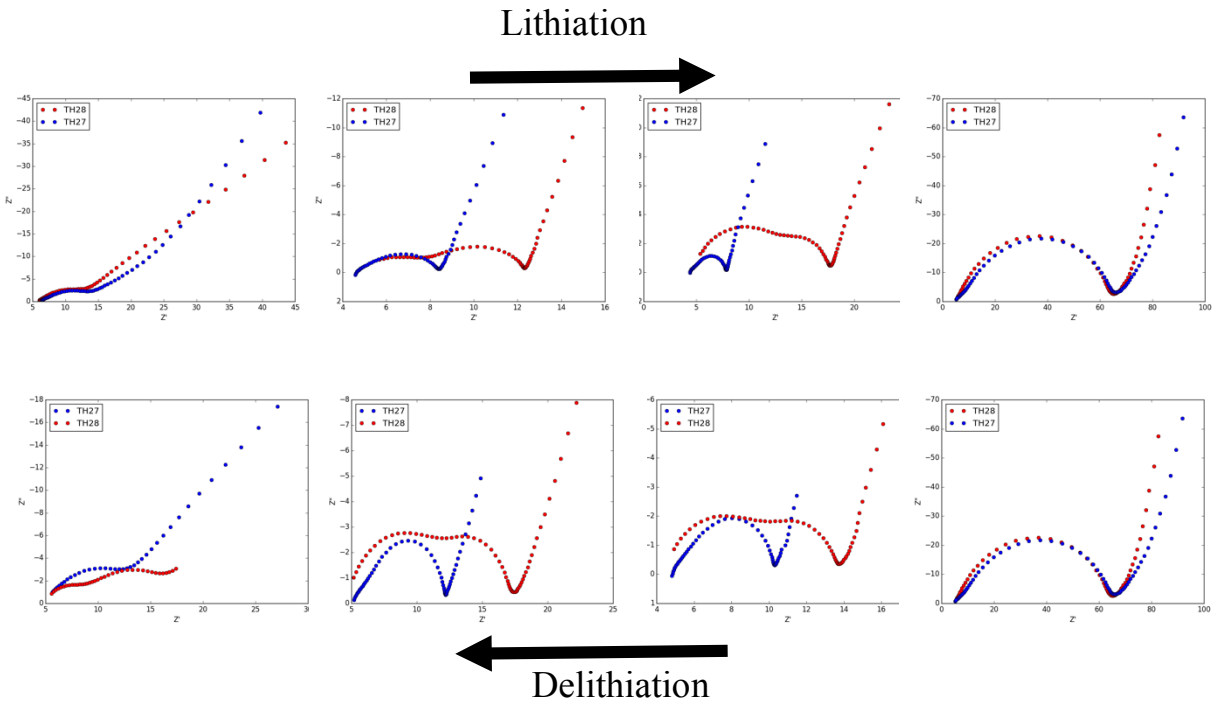

Figure 10: Results of impedance scans during the fifth cycle. Red and blue are two different samples. Note the fully lithiated state is only one scan, repeated for ease of comparison.

Impedance spectra were collected during the fifth cycle on the same samples to monitor impedance changes within a cycle. Scans were taken at the beginning and end of the cycle, and twice during each cycle at about 1/3 and 2/3 capacity through the cycle. The mid-cycle scans were determined by capacity measurement. Figure 10 shows the results of the scans up and down the fifth cycle. The most interesting data is contained in the intermediate scans – the relative values of the two samples are no longer identical. One sample (TH28) has significantly higher impedance during intermediate scans during both the charge and discharge. Another interesting feature of these scans is that there is a secondary RC semicircle in most of the scans. Since this second feature is not present in the initial scans shown in Figure 9, it is likely that this is an impedance from either a phase boundary within the nanowires or the SEI layer. It is also possible that during lithiation the contact resistance to the metal foil becomes significant and creates another semicircle. Further

testing will have to be conducted to determine if the impedance variation is within experimental noise or if there is something fundamentally different about the two samples.

Nanowire synthesis

Throughout the early phase of research, all of the testing was conducted on germanium nanowires, though studying silicon nanowires was more attractive. Problems with silicon synthesis using newer protocols made it difficult to acquire a good sample. In order to use a stable and well understood synthesis process, it was necessary to set up the supercritical fluid reactor to synthesize silicon nanowires. A test synthesis was run using the conditions identified in Richards et al., using 340 mM phenylsilane as a precursor at 5000 psi and 500°C. Four coin cell sized pieces of 100 nm copper on stainless steel (5/8" diameter circles) were used as growth substrate. The samples were placed in the reactor with two at either end of the reactor, none were pushed very far into the center.

Two of the samples exhibited nanowires growth, and the other two samples seem to nanostructure but different from the expected nanowires. The loading on the non-nanowire nanostructure samples was also about half of the other samples, 0.2 mg/cm^2 vs 0.4 mg/cm^2. The two samples with lower loading were at the opposite end of the reactor from the good samples. However, which side they were on was not tracked and isn't known at this time. It is possible that one side was as a slightly higher temperature or had slightly higher precursor concentration. One sample of this batch was successfully built into a

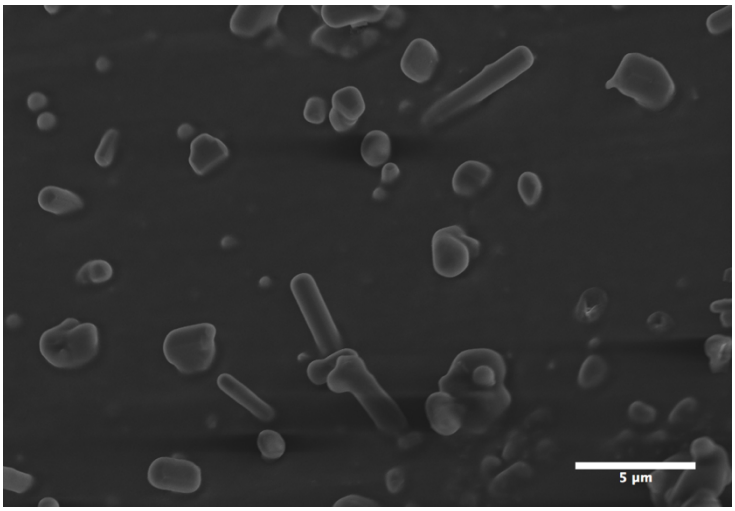

Figure 11: Common morphology for failed nanowire synthesis samples

battery, however the significant curve imparted to the samples by the reactor made it difficult to assemble coin cells. The completed cell had good performance, with an initial capacity of 2200 mAh/g and a capacity of 1000 mAh/g after 20 cycles.

Although the first synthesis was successful, many subsequent syntheses failed to produce nanowires. Many different conditions were used to attempt to replicate the initial success. Resulting morphology typically is similar to what is shown in Figure 11, and loadings were very low, on the order of 0.05 mg/cm^2. Common conditions for the majority reactions include 500˚C, and 340 mM phenylsilane. The pressures used was 5000psi in the 5mL reactor and 3700 psi in the 10 mL reactor. Several theories for why the synthesis was not working were proposed, chiefly related to problems with the substrate or with precursor delivery.

To narrow down the problem with silicon nanowire synthesis, experiments were run to separate problems with the substrate from problems with the experimental apparatus. First, a silicon nanowires synthesis was conducted used a 100nm film of gold instead of copper. Identical conditions to prior experiments were used (340 mM phenylsilane, 3700 psi, 500°C, 10mL reactor).

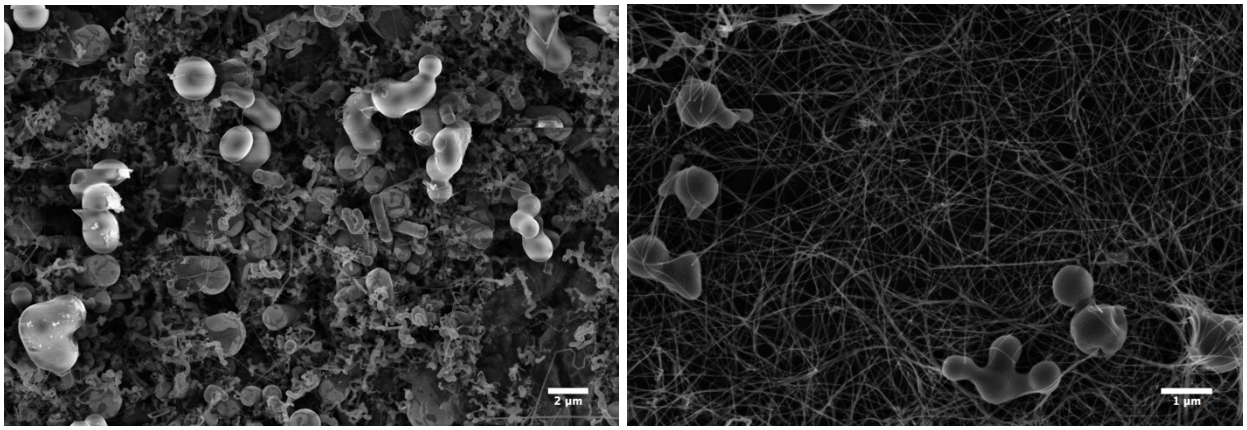

Figure 12: Silicon nanostructure grown on a 100nm gold film (left). Germanium nanowires grown on a 100nm copper film (right).

Silicon and gold have a very low eutectic temperature; at the temperature of the reaction they combine to form a liquid seed. With a very thick film of 100 nanometers, seeds are expected to be of a variety of sizes, ranging from a few nanometers up to a micron. A germanium nanowire synthesis is run under similar conditions to silicon, but with a 600 mM diphenylgermane and at 400°C. Results of these syntheses are shown in Figure 12. The synthesis with a gold film demonstrated the expected morphology for a 100nm film of gold, and the germanium nanowire synthesis successfully produced nanowires. These two results indicated that the precursor was reaching the substrate, and that the reactor was maintaining the appropriate temperature. The problem with the silicon nanowire synthesis, therefore, was believed to be a problem with the copper substrate. The most likely problems with the substrate were air exposure or copper purity.

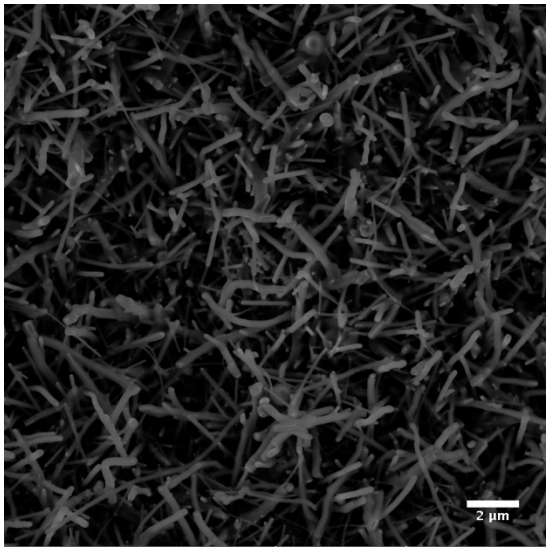

Figure 13: Silicon nanowires on copper stored in the glove box

To determine whether the inhibition to growth is the purity of copper (99.9 vs 99.999% purity) or air exposure, a silicon nanowire synthesis was conducted using two different copper samples prepared and stored in the glove box. Under the same conditions used in previous syntheses, this silicon nanowire synthesis resulted in nanowire formation on both samples. The morphologies were similar for both the 99.9% and the 99.999% purity, indicating that the copper purity is not likely to be a significant contributor to synthesis quality. The resulting nanowires in this synthesis indicate that air exposure of the copper substrate prior to silicon nanowire synthesis is critical in

nanowire formation, SEM of the nanowires in Figure 13. Care will have to be taken to avoid air exposure of substrated, reactor system, and solvents during future syntheses. The first synthesis conducted in October 2015 does not match this conclusion, however, as that copper was not stored in the glove box and nanowires were still formed. It may be possible to reduce the copper using forming gas at high temperature to remove any contaminants or oxide layer formed during air exposure. Several attempts were made at flowing forming gas through the supercritical fluid reactor to clean the copper, and although some progress was made a satisfactory condition has not been identified.

Nanowire synthesis on nickel foams

To grow nanowires on a nickel foam, a catalyst layer must first be deposited. The easiest way to deposit a catalyst layer is through electrodeposition, which can easily be accomplished with a copper sulfate solution. Initially, the copper deposited primarily around the cut edges, indicating that there was an oxide layer that slowed deposition over the majority of the foam. Soaking the

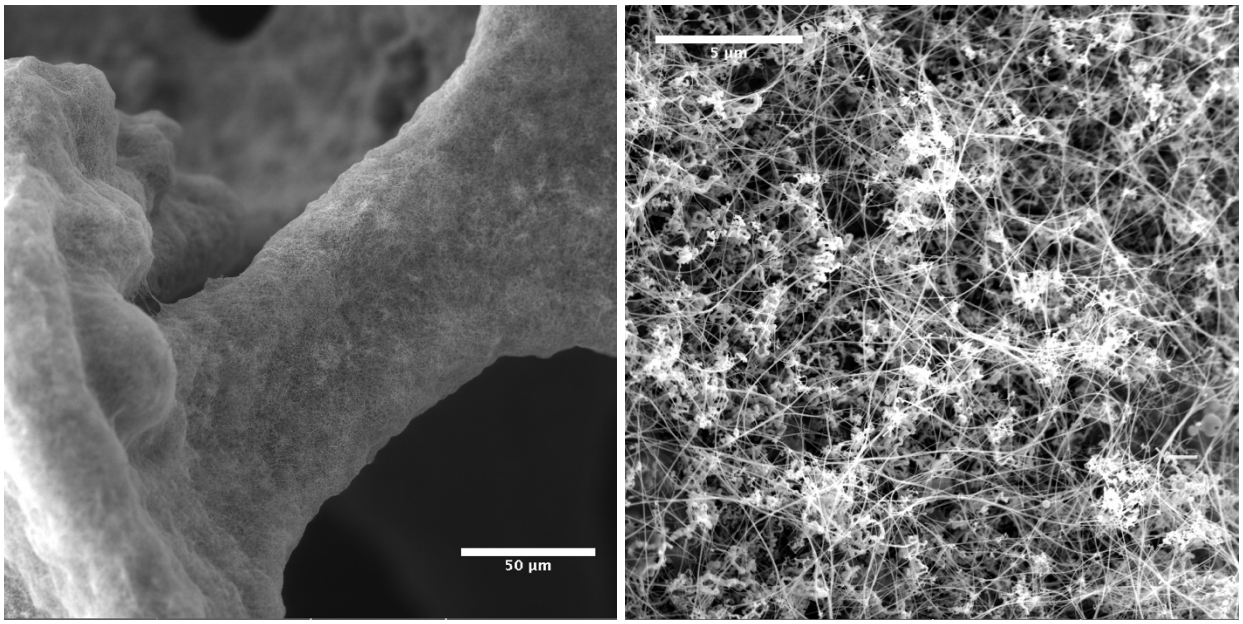

Figure 14: Germanium nanowires on a copper plated nickel foam. The left image provides a wider view of the macroscale features of the nickel foam, the right image shows the nanostructure.

nickel foam for several minutes in 0.1M nitric acid to remove the oxide layer allowed for much more uniform deposition. Copper was deposited using a potentiostat in a 0.1M $CuSO_4$ solution with 0.1M H_2SO_4 as a supporting electrolyte. Using another piece of nickel foam as the counter electrode, a large piece of nickel foam as the working electrode, copper was deposited by applying a pulsed potential of 0.2V vs a Ag/AgCl reference electrode. These conditions resulted in extremely uniform deposition of copper over the whole surface of the nickel foam.

Although a silicon nanowire hierarchal structure has more promise as a potential battery electrode, germanium nanowire synthesis is more robust and provides a good proof of concept. Using the copper coated nickel foam, a supercritical germanium nanowire synthesis was conducted using the same conditions as described above (600mM diphenylgermane, 10 mL reactor, 3700 psi, 400°C). The synthesis covered the entire surface of the foam with a film of high quality very uniform nanowires, at a loading of 5 mg/cm^2. As a control, a piece of non-copper coated nickel foam was included in the synthesis. The no catalyst layer piece did gain some mass, but not a significant amount compared to the foam with copper. Figure 14 shows images of the germanium nanowires on a nickel foam at a different levels of magnification.

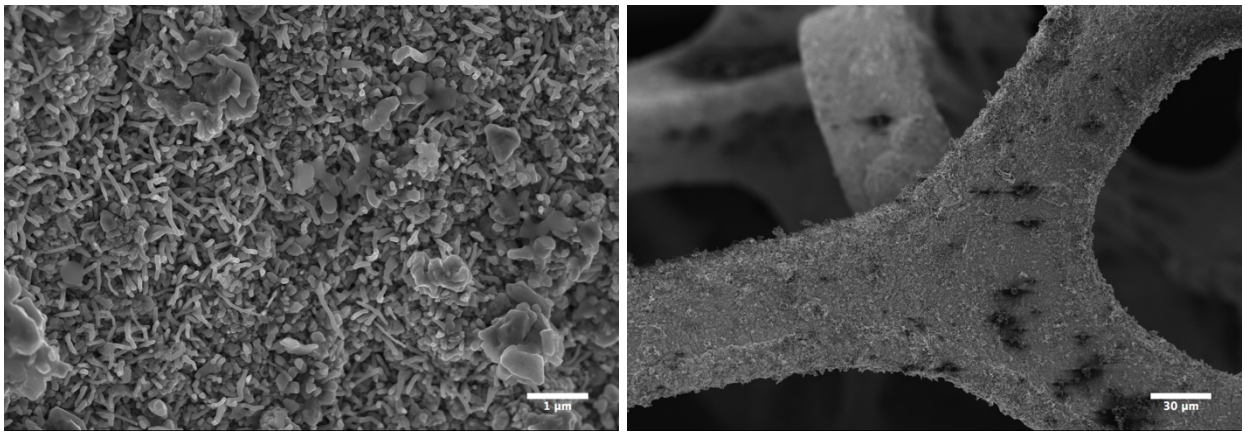

Figure 15: SEM images of silicon nanostructures grown on copper coated nickel foam. Left image depicts a more magnified view of the same area in the right image.

A silicon electrode would present a more attractive substrate for electrochemical study, but the copper coated nickel foams must be air exposed prior to nanowire synthesis. Earlier, it was shown that air exposure significantly impacts nanowire synthesis. Several syntheses were tried using forming gas prior to precursor injection. Samples of planar copper, one which was air exposed and another which was stored in the glove box, in addition to pieces of copper plated nickel foam were placed in the reactor. The reactor was heated to 500°C while flowing forming gas over the substrates at a low sccm flow rate for several hours. After the reduction, the reactor was filled with benzene and the synthesis proceeded as usual. Results of the synthesis can be seen in Figure 15. There was some silicon nanowire deposition on all substrates, however the coverage of the foams was not uniform and the control samples did not have as good of a film as in prior Si nanowire syntheses.

Battery performance of nickel foam nanowire electrodes

To evaluate the performance of the substrates in a battery, coin cells were assembled vs Li/Li+ using 1M $LiPF_6$ in 1:1 EC:DEC with a Celgard separator using both planar germanium nanowire samples and germanium nanowires on nickel foams. The cycling performance of planar and three dimensional cells are both shown in Figure 16. There are several issues with both the control planar cells and the three dimensional cell. In the planar cell, the capacity starts at a value very close to the theoretical maximum but decays extremely quickly in the first ten cycles. The three dimensional cell has mediocre initial capacity, but after 15 cycles has electrical contact issues which cause the capacity data to fluctuate. Both of these tests should be repeated to get better data, as these results are both poor enough to distrust.

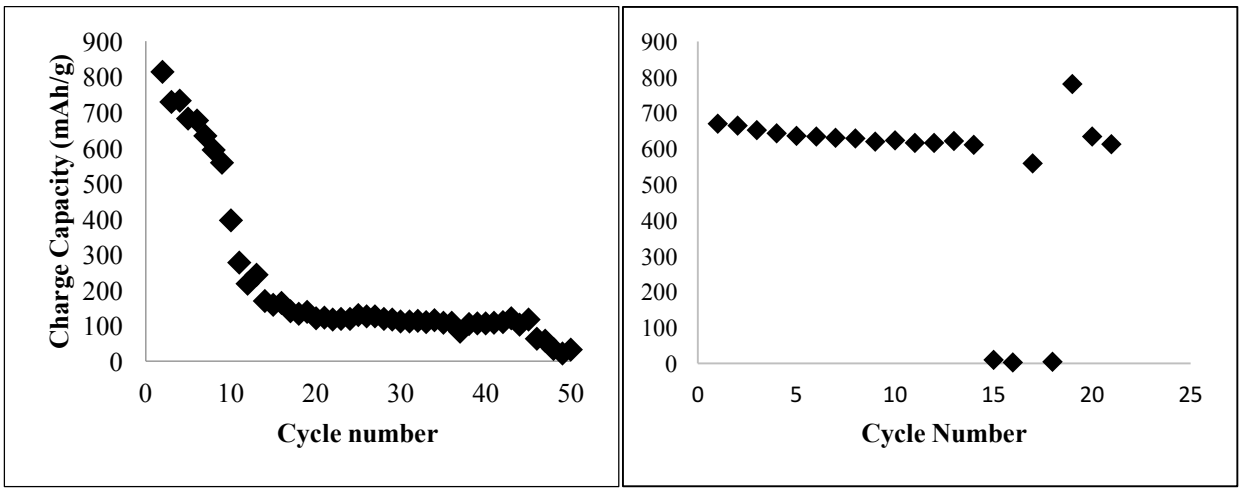

Figure 16: Cycling performance of planar germanium nanowire samples (left) and three dimensional germanium nanowires on copper plated nickel foam.

In addition to cycling testing, the samples rate capabilities were evaluated. The results of the planar and nickel foam samples are shown in Figure 17. The planar sample was tested at 0.1C, 0.2C, 0.5C, and 1C. The foam sample was tested at 0.2C, 0.5C, and 1C. The nanowire sample on the nickel foam and the planar sample show very similar rate performance, with minimal capacity at 1C rate and slightly higher capacity at lower rates. Both samples recovered most of their capacity after returning the initial slower rate. The planar sample recovered less capacity, but it displays a high fade rate which could account for the loss. One possible explanation for the performance being similar is that the pore size of the nanowire foam is not small enough to grant a large increase in kinetic performance. However, the increase in areal loading while maintaining similar performance is an encouraging result.

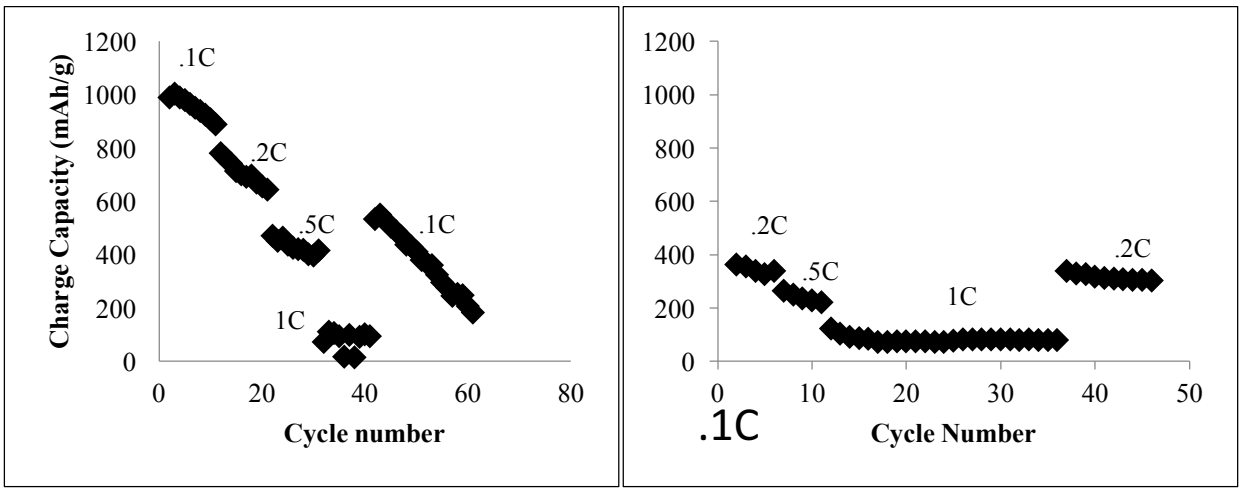

Figure 17: Rate performance of planar (left) and three dimensional germanium nanowire structures

Electrochemical impedance spectroscopy (EIS) was also conducted on two samples, one with planar geometry and another with a nickel foam substrate. The impedance of the nickel foam three dimensional substrate was significant less than that of the planar substrate, indicating more rapid electron transfer through the solution and lower charge transfer resistance. This is indicating by the RC semicircle being closer to zero on the real impedance axis. It is possible that the foam sample had better contact within the battery which would reduce the series resistance. The contact resistance of the planar sample could have been increased because an extremely fragile film was used for these tests. These experiments should be repeated to ensure accuracy and reproducibility of results.

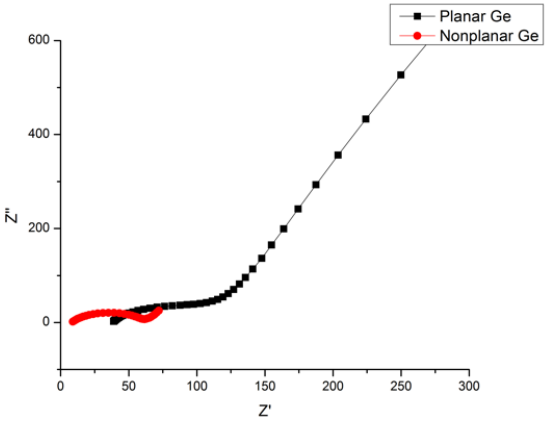

Figure 18: EIS results for planar (blue) and three dimensional (red) samples

CONCLUSIONS

Supercritical fluid synthesis of germanium nanowires in benzene using DPG has proven to be a robust process at a wide variety of temperatures. Even with air exposed copper, germanium nanowires are formed on a copper film in supercritical benzene using DPG as a precursor. The high diffusivity and low surface tension of supercritical fluids allows the precursor to reach the surface uniformly, differing from gas phase conditions where the outer edges have higher loading. Hierarchal structures of germanium nanowires on nickel foams were successfully synthesized with high loading and uniform coverage of germanium nanowires. However, synthesis of silicon nanowires on a nickel foam requires further study of reducing any contamination of the copper surface resulting from air exposure. The electrochemical performance of the samples was not excellent, but further testing could be completed to improve the performance. On possible reason for reduced capacity in early cycles is wire breakage. To prevent wire breakage during experiment, the wires could be carbon coated or built using a slurry with conductive carbon. The slurry cell would maintain electrical contact even if the wires break, removing that as a factor for capacity loss. To extend and further complete the work on hierarchal nanowire structures, of primary importance are improving electrochemical performance of germanium films and creating hierarchal structures with silicon nanowires.

REFERENCES

1. Goodenough, J. B. & Kim, Y. Challenges for Rechargeable Li Batteries †. *Chem. Mater.* **22,** 587–603 (2010).
2. Hayner, C. M., Zhao, X. & Kung, H. H. Materials for Rechargeable Lithium-Ion Batteries. *Annu. Rev. Chem. Biomol. Eng.* **3,** 445–471 (2012).
3. Chan, C. K. *et al.* High-performance lithium battery anodes using silicon nanowires. *Nature Nanotechnology* **3,** 31–35 (2007).
4. Chockla, A. M., Klavetter, K. C., Mullins, C. B. & Korgel, B. A. Solution-Grown Germanium Nanowire Anodes for Lithium-Ion Batteries. *ACS Appl. Mater. Interfaces* **4,** 4658–4664 (2012).
5. Su, X. *et al.* Silicon-Based Nanomaterials for Lithium-Ion Batteries: A Review. *Adv. Energy Mater.* **4,** n/a–n/a (2013).
6. Liu, X. H. *et al.* In Situ TEM Experiments of Electrochemical Lithiation and Delithiation of Individual Nanostructures. *Adv. Energy Mater.* **2,** 722–741 (2012).
7. Fuller, C. S. & Severiens, J. C. Mobility of Impurity Ions in Germanium and Silicon. *Phys. Rev.* **96,** 21–24 (1954).
8. Weydanz, W. J., Wohlfahrt-Mehrens, M. & Huggins, R. A. A room temperature study of the binary lithium–silicon and the ternary lithium–chromium–silicon system for use in rechargeable lithium batteries. *Journal of Power Sources* **81-82,** 237–242 (1999).
9. Bloom, I. *et al.* Differential voltage analyses of high-power lithium-ion cells. 4. Cells containing NMC. *Journal of Power Sources* **195,** 877–882 (2010).
10. Verma, P., Maire, P. & Novák, P. A review of the features and analyses of the solid electrolyte interphase in Li-ion batteries. *Electrochimica Acta* **55,** 6332–6341 (2010).
11. Nie, M., Abraham, D. P., Chen, Y., Bose, A. & Lucht, B. L. Silicon Solid Electrolyte Interphase (SEI) of Lithium Ion Battery Characterized by Microscopy and Spectroscopy. *J. Phys. Chem. C* **117,** 13403–13412 (2013).
12. Wu, H. & Cui, Y. Designing nanostructured Si anodes for high energy lithium ion batteries. *Nano Today* **7,** 414–429 (2012).
13. Liu, N. *et al.* A pomegranate-inspired nanoscale design for large-volume-change lithium battery anodes. *Nature Nanotechnology* **9,** 187–192 (2014).
14. Kim, J. S., Byun, D. & Lee, J. K. Electrochemical characteristics of amorphous silicon thin film electrode with fluoroethylene carbonate additive. *Current Applied Physics* (2014). doi:10.1016/j.cap.2014.02.008
15. McDowell, M. T. *et al.* Novel Size and Surface Oxide Effects in Silicon Nanowires as Lithium Battery Anodes. *Nano Lett.* **11,** 4018–4025 (2011).
16. Cho, J.-H. & Picraux, S. T. Silicon Nanowire Degradation and Stabilization during Lithium Cycling by SEI Layer Formation. *Nano Lett.* **14,** 3088–3095 (2014).
17. Choi, N.-S. *et al.* Effect of fluoroethylene carbonate additive on interfacial properties of silicon thin-film electrode. *Journal of Power Sources* **161,** 1254–1259 (2006).
18. Li, J., Xiao, X., Cheng, Y.-T. & Verbrugge, M. W. Atomic Layered Coating Enabling Ultrafast Surface Kinetics at Silicon Electrodes in Lithium Ion Batteries. *J. Phys. Chem. Lett.* **4,** 3387–3391 (2013).

19. Bogart, T. D. *et al.* Lithium Ion Battery Peformance of Silicon Nanowires with Carbon Skin. *ACS Nano* **8,** 915–922 (2014).
20. Zamfir, M. R., Nguyen, H. T., Moyen, E., Lee, Y. H. & Pribat, D. Silicon nanowires for Li-based battery anodes: a review. *J. Mater. Chem. A* **1,** 9566–21 (2013).
21. Wen, C. J. & Huggins, R. A. Chemical diffusion in intermediate phases in the lithium-silicon system. *Journal of Solid State Chemistry* **37,** 271–278 (1981).
22. Chan, C. K., Patel, R. N., O'Connell, M. J., Korgel, B. A. & Cui, Y. Solution-Grown Silicon Nanowires for Lithium-Ion Battery Anodes. *ACS Nano* **4,** 1443–1450 (2010).
23. Wagner, R. S. & Ellis, W. C. VAPOR-LIQUID-SOLID MECHANISM OF SINGLE CRYSTAL GROWTH. *Appl. Phys. Lett.* **4,** 89 (1964).
24. Morales, A. M. A Laser Ablation Method for the Synthesis of Crystalline Semiconductor Nanowires. *Science* **279,** 208–211 (1998).
25. Lieber, C. M., Hu, J., Ouyang, M. & Yang, P. Controlled growth and electrical properties of heterojunctions of carbon nanotubes and silicon nanowires. *Nature* **399,** 48–51 (1999).
26. Mullane, E., Kennedy, T., Geaney, H. & Ryan, K. M. A Rapid, Solvent-Free Protocol for the Synthesis of Germanium Nanowire Lithium-Ion Anodes with a Long Cycle Life and High Rate Capability. *ACS Appl. Mater. Interfaces* **6,** 18800–18807 (2014).
27. Yuan, F.-W., Yang, H.-J. & Tuan, H.-Y. Seeded silicon nanowire growth catalyzed by commercially available bulk metals: broad selection of metal catalysts, superior field emission performance, and versatile nanowire/metal architectures. *Journal of Materials Chemistry* **21,** 13793–13800 (2011).
28. Richards, B. T. *et al.* Direct growth of germanium and silicon nanowires on metal films. *J. Mater. Chem. C* **2,** 1869–1878 (2014).
29. Peled, E. *et al.* Tissue-like Silicon Nanowires-Based Three-Dimensional Anodes for High-Capacity Lithium Ion Batteries. *Nano Lett.* 150518105731007–10 (2015). doi:10.1021/acs.nanolett.5b00744
30. Lin, Y.-M. *et al.* High performance silicon nanoparticle anode in fluoroethylene carbonate-based electrolyte for Li-ion batteries. *Chem. Commun.* **48,** 7268 (2012).
31. Chockla, A. M. *et al.* Influences of Gold, Binder and Electrolyte on Silicon Nanowire Performance in Li-Ion Batteries. *J. Phys. Chem. C* **116,** 18079–18086 (2012).
32. Martin, L., Martinez, H., Ulldemolins, M., Pecquenard, B. & Le Cras, F. Evolution of the Si electrode/electrolyte interface in lithium batteries characterized by XPS and AFM techniques: The influence of vinylene carbonate additive. *Solid State Ionics* **215,** 36–44 (2012).
33. Kennedy, T. *et al.* High-Performance Germanium Nanowire-Based Lithium-Ion Battery Anodes Extending over 1000 Cycles Through in Situ Formation of a Continuous Porous Network. *Nano Lett.* **14,** 716–723 (2014).
34. Lee, G.-H., Lee, S., Lee, C. W., Choi, C. & Kim, D.-W. Stable high-areal-capacity nanoarchitectured germanium anodes on three-dimensional current collectors for Li ion microbatteries. *Journal of Materials Chemistry A: Materials for energy and sustainability* **4,** 1060–1067 (2015).
35. Yang, Y., Cheng, D., Chen, S., Guan, Y. & Xiong, J. Construction of Hierarchical

NiCo2S4@Ni(OH)2 Core-Shell Hybrid Nanosheet Arrays on Ni Foam for High-Performance Aqueous Hybrid Supercapacitors. *Electrochimica Acta* **193,** 116–127 (2016).
36. Han, Z. *et al.* Donut-shaped Co3O4 nanoflakes grown on nickel foam with enhanced supercapacitive performances. *Applied Surface Science* **365,** 240–244 (2016).
37. Ruffo, R., Hong, S. S., Chan, C. K., Huggins, R. A. & Cui, Y. Impedance Analysis of Silicon Nanowire Lithium Ion Battery Anodes. *J. Phys. Chem. C* **113,** 11390–11398 (2009).
38. Song, J. & Bazant, M. Z. Effects of Nanoparticle Geometry and Size Distribution on Diffusion Impedance of Battery Electrodes. *Journal of the Electrochemical Society* **160,** A15–A24 (2012).
39. Silberstein, K. E. *et al.* OperandoX-ray Scattering and Spectroscopic Analysis of Germanium Nanowire Anodes in Lithium Ion Batteries. *Langmuir* **31,** 2028–2035 (2015).